ARTICLE

OBC
www.rsc.org/obc

4-(Tetrahydro-4*H*-thiopyran-1-oxide-4-ylidene)-cyclohexanone oxime in the solid-state. A two-dimensional network of enantiomorphous chains interconnected by weak hydrogen bonds†

Albert W. Marsman,[a] Bart L. A. van Poecke,[a] Leonardus W. Jenneskens,*[a] Anthony L. Spek,[b] Egbertus T. G. Lutz[c] and Joop H. van der Maas[c]

[a] *Debye Institute, Organic Chemistry and Catalysis, Utrecht University, Padualaan 8, 3584 CH, Utrecht, The Netherlands. E-mail: l.w.jenneskens@chem.uu.nl; Fax: +31 30 2534533; Tel: +31 30 2533128*

[b] *Bijvoet Center for Biomolecular Research, Crystal and Structural Chemistry, Utrecht University, Padualaan 8, 3584 CH, Utrecht, The Netherlands*

[c] *Department of Vibrational Spectroscopy, Utrecht University, Sorbonnelaan 16, 3584 CA, Utrecht, The Netherlands*

Received 12th January 2005, Accepted 24th February 2005
First published as an Advance Article on the web 16th March 2005

From a saturated C_6H_6 solution of racemic 4-(tetrahydro-4*H*-thiopyran-1-oxide-4-ylidene)-cyclohexanone oxime [**1** (**1**-*R*/**1**-*S*)] the co-crystal **(1)$_4$·C$_6$H$_6$** is crystallized. Single crystal X-ray analysis showed that **(1)$_4$·C$_6$H$_6$** ($P\bar{1}$ space group) in the solid-state consists of enantiomorphous, non-covalent polymer-like chains that contain, in an alternating fashion, the crystallographically independent enantiomers **1**-*R* and **1**-*R*′ or **1**-*S* and **1**-*S*′, respectively. Within each chain the enantiomers are linked by '*head-to-tail*' intermolecular oxime–sulfoxide hydrogen bonding [D(2) motif]. Neighbouring chains consist of enantiomers with opposite configuration and possess opposite molecular '*head-to-tail*' alignments. The enantiomorphous chains are interconnected by weak intermolecular C–H · · · O hydrogen bonds involving centrosymmetric C–H · · · oxime [$R_2^2(12)$] and C–H · · · sulfoxide [$R_2^2(8)$] motifs between the **1**-*R* and **1**-*S* molecules in neighbouring chains; a nearly planar two-dimensional hydrogen bonding network motif is obtained. In the crystallographic direction [1 0 0] the layers stack in such a fashion that chains occupying successive layers with an identical '*head-to-tail*' alignment are positioned on top of each other. Concomitantly, channels with areas of *ca.* 25 Å^2 are obtained, which are occupied by C_6H_6 solvent molecules. A comparison of the IR and Raman spectra of **(1)$_4$·C$_6$H$_6$** with those obtained for native **1** that does not contain C_6H_6, indicates that intermolecular oxime–sulfoxide hydrogen bonding [D(2) motif] also occurs for native **1** in the solid-state.

Introduction

Directional intermolecular hydrogen bonding is extensively used for the preparation of supramolecular systems and crystal engineering.[1] In previous papers we have reported on the assembly of semi-rigid rod-like oligo(cyclohexylidenes) and their saturated analogues, consisting of cyclohexyl-type rings connected *via* their 1 and 1′ positions by either olefinic or single carbon–carbon bonds, which bear either one or two oxime [–C(R)=N–OH] end groups.[2] Single crystal X-ray analyses revealed that oligo(cyclohexylidene) mono- and bis-oximes form linear rod-like dimers and infinite, non-covalent polymer-like chains,[3] respectively, *via* self-complementary intermolecular dimeric oxime hydrogen bonding[4] [graph set notation: $R_2^2(6)$ motif[5]]. Since the oxime O–H moiety may occupy two positions with respect to the C–C=N plane due to the high barrier for nitrogen inversion in oximes ($\Delta H^{\ddagger} = 167.4$–$209.2$ kJ mol^{-1}),[6] the mono- as well as bis-oximes consist of mixtures of stereoisomers. Besides the occurrence of *E*/*Z*-stereoisomerism in the case of the bis-oximes, many of the oligo(cyclohexylidene) mono- and bis-oximes are axially dissymmetric, *i.e.* they possess a chiral axis parallel to the imino bond.[3] For these derivatives we have shown that upon crystallization of the racemate intermolecular dimeric oxime, hydrogen bonding [$R_2^2(6)$ motifs] exclusively occurs between enantiomers or enantiomeric molecular subunits of opposite configuration.

However, crystallization of *E*-(*E*-**6**) and *Z*-1,1′-bicyclohexylidene-4,4′-dione bis-oxime (*Z*-**6**, ratio *E* : *Z* 1 : 1, Scheme 1) from a C_6H_6–DMSO (*v*/*v* 1 : 1) solution gave co-crystals which exclusively consist of *E*-**6** and DMSO in a ratio of 1 : 2 [*E*-**6**·**(DMSO)$_2$**], in which each oxime moiety is hydrogen bonded to a sulfoxide group (Fig. 1).[3c] To our knowledge this is the only reported example (Cambridge Crystallographic Database) in which intermolecular oxime–sulfoxide hydrogen bonding [graph set notation: D(2) motif[5]] is encountered. More importantly, it shows that intermolecular oxime–sulfoxide hydrogen bonding is favoured over intermolecular dimeric oxime hydrogen bonding.

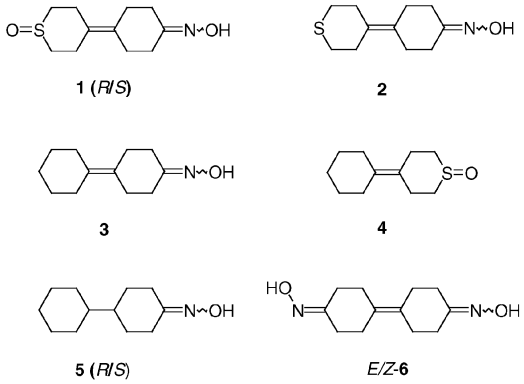

Scheme 1 Compounds **1**–**6**.

† Electronic Supplementary Information (ESI) available: PM3 archive files for an enantiomer of **1**, *viz.* **1**-*R*, with its bicyclohexylidene skeleton in either a *syn*- or *anti*-conformation. See http://www.rsc.org/suppdata/ob/b5/b500527b

DOI: 10.1039/b500527b

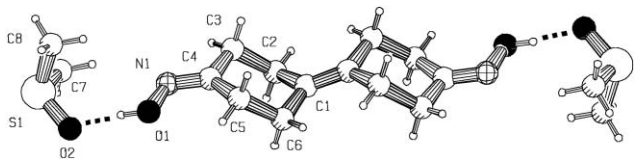

Fig. 1 Co-crystals of the *E*-**6** and DMSO, *viz.* *E*-**6**·**(DMSO)$_2$**. Selected bond lengths (in Å), valence angles (in °) and torsion angles (in °): N1–O1 1.4090(18), O1–O2 2.6529(17), S1–O2 1.5609(13), N1–O1 ··· O2 99.12(8), S1–O2 ··· O1 122.69(7), S1–O2 ··· O1—N1 −54.94(11).[3c]

This was attributed to the strong hydrogen bond acceptor properties of sulfoxides.[3c]

This result has prompted us to synthesize another bicyclohexylidene derivative, *viz.* 4-(tetrahydro-4*H*-thiopyran-1-oxide-4-ylidene)-cyclohexanone oxime (**1**, Scheme 1), which contains an oxime functionality at one end-position and a sulfoxide functionality at the other end-position. The objective is to investigate the propensity of **1** towards molecular recognition, *e.g.* the occurrence of selective intermolecular oxime–sulfoxide hydrogen bonding in the solid-state and in solution. Note that the configurational properties of the oxime and the sulfoxide moiety render **1** axial dissymmetric, *i.e.* **1** will be present as an enantiomer pair (**1**-*R*/**1**-*S*, *vide infra*).

Here we report the single crystal X-ray structure of the co-crystal **(1)$_4$·C$_6$H$_6$**, in which all molecules of **1** are linked by '*head-to-tail*' intermolecular oxime–sulfoxide hydrogen bonding [D(2) motifs] into infinite, non-covalent polymer-like chains. Each distinct chain contains only one enantiomer, *viz.* **1**-*R* (**1**-*R*′) or **1**-*S* (**1**-*S*′). The chains are interconnected by weak hydrogen bond interactions furnishing planar two-dimensional networks that stack on top of each other, leading to the formation of channels that contain the C_6H_6 molecules.

The occurrence and nature of intermolecular hydrogen bonding in the solid-state of native **1**, which does not contain C_6H_6, was assessed using IR and Raman spectroscopy. A comparison of the spectral data of **(1)$_4$·C$_6$H$_6$** with those of native **1** and the reference compounds **2–5** (Scheme 1) indicates that **(1)$_4$·C$_6$H$_6$** and **1** possess similar strong intermolecular hydrogen bonding motifs.

Results and discussion

Synthesis of 1–5

4-(Tetrahydro-4*H*-thiopyran-1-oxide-4-ylidene)cyclohexanone oxime (**1**) and 4-(tetrahydro-4*H*-thiopyran-4-ylidene)cyclohexanone oxime (**2**) were obtained as crystalline compounds from the ketones **8** and **9**[3] (Scheme 2 and see Experimental). Compound **8** was converted into **9** by oxidation following the same procedure as applied for 4-cyclohexylidene-tetrahydro-4*H*-thiopyran-1-oxide (**4**).[7] 1,1′-Bicyclohexylidene-4-one oxime (**3**)[3] and 4-cyclohexylcyclohexanone oxime (**5**)[8] were available from previous studies.

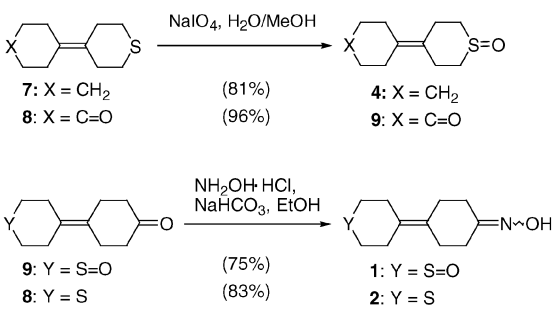

Scheme 2 Synthesis of compounds **1–2** and **4**.

Since the oxime and sulfoxide moieties of **1** are oriented nearly perpendicular with respect to each other and nitrogen inversion in oximes[6] as well as sulfur inversion in sulfoxides is restricted,[9] **1** is axially dissymmetric, *e.g.* **1** possesses a chiral axis parallel to the imino bond (Fig. 2).[10,11] The presence of an enantiomer pair (**1**-*R*/**1**-*S*, Fig. 3) was unequivocally established using chiral HPLC.

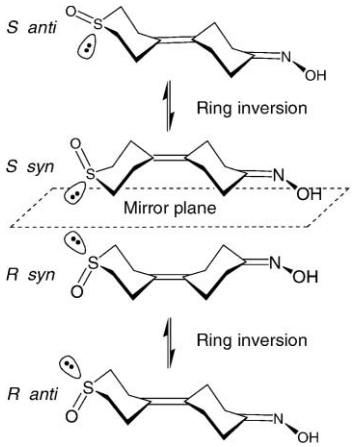

Fig. 2 Possible enantiomers of **1** (**1**-*R*/**1**-*S*). Note that inversion of the cyclohexyl-type rings does not affect the absolute configuration of the enantiomers (*cf.* text).

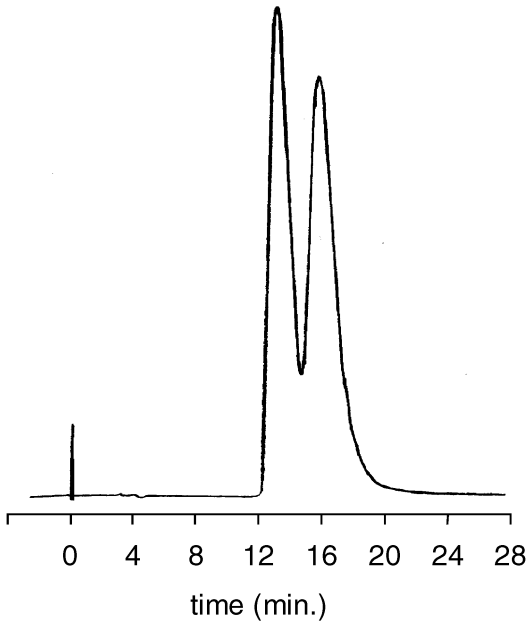

Fig. 3 Chiral HPLC trace of racemic native **1** (**1**-*R*/**1**-*S*).‡

Stereoisomerism of 1

Notwithstanding, **1** still may adopt different conformations in solution (Fig. 2). Temperature dependent ^{1}H NMR (DMSO-d_6, temperature range 25–147 °C) of native **1** and the reference compound 4-cyclohexylidene-tetrahydro-4*H*-thiopyran-1-oxide (**4**) revealed that the proton coupling patterns of the cyclohexyl-type ring bearing the sulfoxide moiety change, indicating that these rings possess restricted conformational flexibility. ^{1}H NMR investigations on tetrahydro-4*H*-thiopyran-1-oxide and its alkyl-substituted analogues revealed the occurrence of temperature dependent equilibria between conformers with axial and equatorial sulfoxide groups and that an axial sulfoxide moiety is preferred.[12] Hence, conformers of **1** with sulfoxide groups in

‡ With the exception of an additional peak for C_6H_6 (t_R = 4.5 min.), the chiral HPLC trace of **(1)$_4$·C$_6$H$_6$** is identical.

an axial position are expected to predominate in solution. In contrast, the cyclohexyl-type rings of **1** and **2** that contain the oxime group, like those of 1,1′-bicyclohexylidene-4-one oxime (**3**) and 1,1′-bicyclohexylidene-1,4′-dione bis-oxime (*E*/*Z*-**6**), are conformationally flexible under similar conditions (Scheme 1).[3] Semi-empirical PM3[13] calculations on one of the enantiomers of *syn*- and *anti*-**1** with an axial sulfoxide group, *viz.* **1**-*R* (Fig. 2), gave enthalpies of formation [$\Delta H°_f$(*syn*-**1**) −141.0 kJ mol^{-1} and $\Delta H°_f$(*anti*-**1**) −139.3 kJ mol^{-1}].† This suggests the presence of a conformational equilibrium in solution (*anti*-**1** : *syn*-**1** of 1 : 2). Similar equilibrium ratios were found between the *anti*- and *syn*-conformers of 1,1′-bicyclohexylidene-1,4′-dione bis-oxime (*E*/*Z*-**6**)[3d] and 1,1′-bicyclohexylidene.[14] In passing, we note that the conformational properties of the cyclohexyl-type rings do not affect the absolute configuration of **1**-*R* and **1**-*S* (*cf.* Fig. 2).

Single crystal X-ray structure of $(\mathbf{1})_4\cdot\mathbf{C_6H_6}$

To gain insight in the occurrence of intermolecular hydrogen bonding of racemic **1** (**1**-*R*/**1**-*S*) in the solid-state, a suitable single crystal obtained from slow cooling of a hot saturated C_6H_6 solution was subjected to X-ray analysis. The crystal has the achiral $P\bar{1}$ space group with a unit cell containing two crystallographically independent enantiomer pairs **1**-*R*/**1**-*S* and **1**-*R*′/**1**-*S*′, Fig. 4 and see Experimental). In addition, each unit cell also contains one molecule C_6H_6, *i.e.* a co-crystal of composition $\mathbf{(1)_4\cdot C_6H_6}$ is obtained. The cyclohexyl-type ring (C1–C6, Fig. 4) bearing the oxime group of one of the two crystallographically independent enantiomer pairs of **1** (**1**-*R*′/**1**-*S*′) as well the incorporated C_6H_6 solvent molecules that occupy the channels are slightly disordered leading to a higher *R*-factor (10%, see Experimental). As will be discussed, the disorder in **1**-*R*′/**1**-*S*′ is due to the absence of additional, weak intermolecular hydrogen bonds between **1**-*R*′ and **1**-*S*′ in neighbouring chains that interconnect the other crystallographically independent enantiomers **1**-*R* and **1**-*S*, respectively.

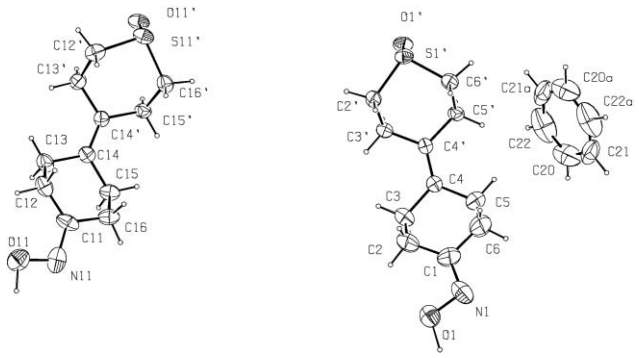

Fig. 4 Displacement ellipsoid plot of $\mathbf{(1)_4\cdot C_6H_6}$ (50% probability). Selected bond lengths (in Å), valence angles (in °) and torsion angles (in °). Both residues of **1** shown have the *R*-configuration. *Residue 1*: S1′–O1′ 1.517(4), N1–C1 1.333(11), O1–N1 1.381(8), O1–N1–C1 106.6(6). *Residue 2*: S11′–O11′ 1.515(4), N11–C11 1.357(9), O11–N11 1.372(8), O11–N11–C11 107.3(5).

In the solid-state, molecules of **1** are linked by '*head-to-tail*' intermolecular oxime–sulfoxide hydrogen bonding [D(2) motif, Fig. 5]. Unfortunately, the hydrogen atoms of these intermolecular hydrogen bonds could not be unambiguously located, which hampers a detailed analysis. Notwithstanding, two slightly different D(2) motifs are discernible. The intermolecular distances between the sulfoxide oxygen and the oxime oxygen of the hydrogen bonded groups [O1 ⋯ O11′, 2.706(6) Å and O1′ ⋯ O11, 2.729(6) Å] are *ca.* 0.3 Å shorter than the sum of their (atomic) van der Waal's radii.[15] They are slightly longer than the corresponding distance in *E*-$\mathbf{6\cdot(DMSO)_2}$ [2.6529(17) Å].[3c] The geometry of the oxime–sulfoxide hydrogen bonding motifs in $\mathbf{(1)_4\cdot C_6H_6}$ and *E*-$\mathbf{6\cdot(DMSO)_2}$, however, differ (*cf.* Fig. 1, Fig. 4 and Fig. 5).† The oxime O–H group points towards opposite sides of the sulfoxide groups to which they are non-covalently linked (Fig. 1 and Fig. 5).

As a consequence of the '*head-to-tail*' intermolecular oxime–sulfoxide hydrogen bonding pattern, infinite, non-covalent polymer-like chains are formed, which extend in the crystallographic direction [2 1 1] (Fig. 5). In analogy to *E*-$\mathbf{6\cdot(DMSO)_2}$,[3c] the intermolecular oxime–sulfoxide hydrogen-bonding motif is preferred over self-complementary intermolecular oxime–oxime hydrogen bonding in the case of $\mathbf{(1)_4\cdot C_6H_6}$. Within each specific chain only one of the enantiomers of **1** is present, *i.e.* the distinct chains are enantiomorphous and contain the crystallographically independent enantiomers in an alternating **1**-*R* ⋯ **1**-*R*′ (**1**-*S* ⋯ **1**-*S*′) pattern.

Inspection of the solid-state packing motif of $\mathbf{(1)_4\cdot C_6H_6}$ shows the presence of short intermolecular distances between some cyclohexyl-like C–H groups and the oxygen atoms of the oxime and sulfoxide group of one of the crystallographically independent enantiomer pairs [**1**-*R*/**1**-*S* (C13 ⋯ O11§ and C16′ ⋯ O11′*, Fig. 5)]. The short contact distances are indicative of the presence of extra weak C–H ⋯ O hydrogen bond interactions.[16,17] Two weak intermolecular hydrogen bonding motifs are identified, *i.e.* an $R_2^2(12)$ C–H ⋯ oxime motif and a $R_2^2(8)$ C–H ⋯ sulfoxide motif (Fig. 5). Whereas the latter motif is similar to that found in the single crystal X-ray structure of *trans*-1,4-dithian-1,4-dioxide, which adopts a C_s-symmetrical chair conformation with both sulfoxide groups in the axial-position,[18] the intermolecular $R_2^2(12)$ motif is to our knowledge unprecedented. These weak intermolecular hydrogen bonds link all non-covalent polymer-like chains of **1** into a two-dimensional hydrogen bonded network (Fig. 6).[17] Since the $R_2^2(12)$ and $R_2^2(8)$ motifs are centrosymmetric, each enantiomorphous chain within a nearly planar two-dimensional network is complemented by a neighbouring chain of opposite configuration. Since in $\mathbf{(1)_4\cdot C_6H_6}$ the weak C–H ⋯ O interactions exclusively occur between the crystallographically independent enantiomers **1**-*R* and **1**-*S* of neighbouring chains, the absence of similar interactions between the enantiomers **1**-*R*′ and **1**-*S*′ accounts for the observed disorder of their cyclohexyl-type rings bearing the oxime group (C1–C6, Fig. 4).

With respect to the effect of the weak C–H ⋯ O interactions on the conformation of **1**, it is worthwhile to note that, in contrast with all previously reported single crystal X-ray structures of (functionalized) oligo(cyclohexylidenes),[3] the bicyclohexylidene skeleton of **1** possesses a *syn*-conformation, *viz.* a boat-like shape instead of the usual staircase-like shape (*anti*-conformation) is found [*cf.* *E*-$\mathbf{6\cdot(DMSO)_2}$ and Fig. 1, Fig. 4 and Fig. 5].[3c] The sulfoxide group of **1** occupies an axial position (*cf.* reference 18), which is of interest for the formation of the additional $R_2^2(8)$ C–H ⋯ sulfoxide hydrogen bonding motifs. In the crystal structure of $\mathbf{(1)_4\cdot C_6H_6}$ the weak C–H ⋯ O interactions of the intermolecular $R_2^2(12)$ C–H ⋯ oxime hydrogen bonding motif apparently contributes to enforce the *syn*-conformation.

Since the two-dimensional networks of neighbouring chains are nearly planar, stacking of successive planes in the third-dimension (crystallographic direction [1 0 0]) is facilitated (Fig. 6). The enantiomorphous chains positioned on top of each other in successive layers possess an identical molecular '*head-to-tail*' arrangement of alternating **1**-*R* ⋯ **1**-*R*′ or alternating **1**-*S* ⋯ **1**-*S*′. Concomitantly, channels (area *ca.* 25 Å^2) parallel to the stacking direction are obtained, which are occupied by C_6H_6 solvent molecules (Fig. 6).

Solid-state structure of native 1: intermolecular hydrogen bonding motifs

Since native, polycrystalline **1** does not contain C_6H_6, its propensity towards intermolecular hydrogen bonding in the solid-state may differ from that found for $\mathbf{(1)_4\cdot C_6H_6}$. Therefore, native **1**, $\mathbf{(1)_4\cdot C_6H_6}$ and the reference compounds **2–5** (Scheme 1)

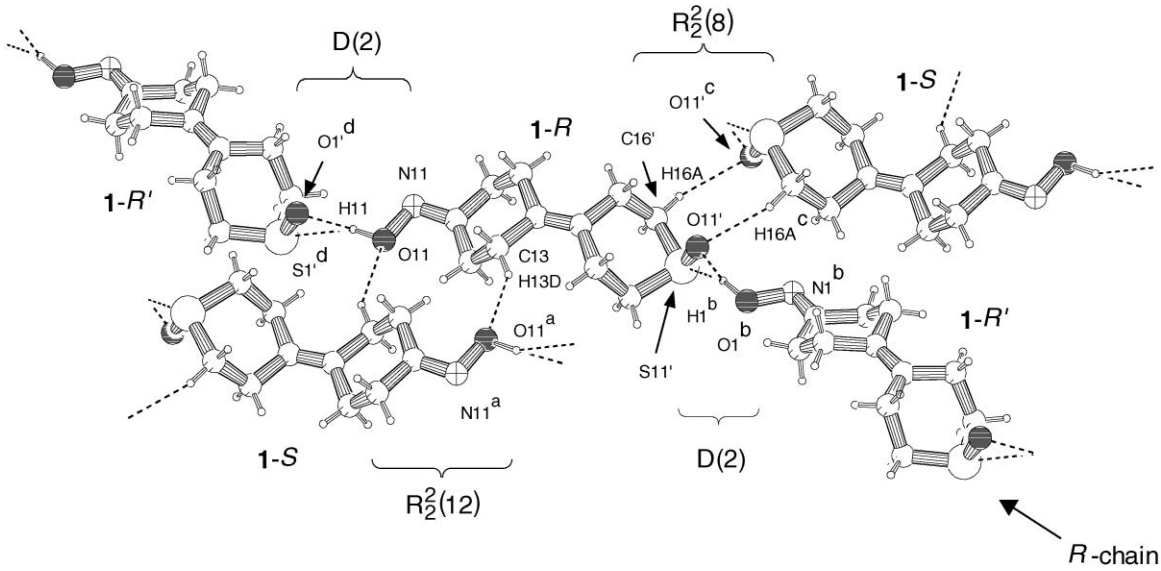

Fig. 5 Intermolecular interactions in **(1)$_4$·C$_6$H$_6$**. A chiral non-covalent polymer-like chain (**1**-*R*) formed due to intermolecular oxime–sulfoxide hydrogen bonding *via* two slightly different D(2) motifs: Hydrogen bonds: S1′††–O1′††···O11 109.6(2)°, S11′–O11′···O1¶ 119.5(3)°, N1¶–O1¶···O11′ 108.8(4)°, N11–O11···O1′†† 109.9(4)°, S1′††–O1′††···O11–N11 99.6(4)°, S11′–O11′···O1¶–N1¶ 92.8(4)°. The chains are interlinked *via* weak secondary intermolecular C–H···O interations according to centrosymmetric C–H···oxime $R_2^2(12)$ and C–H···sulfoxide $R_2^2(8)$ motifs: C13···O11§ 3.406(8) Å, C13–H13D 0.9699 Å, H13D···O11§ 2.5739 Å, C13–H13D···O11§ 143.89°, C16′···O11′* 3.373(6) Å, C16′–H16A 0.9705 Å, H16A···O11′* 2.4338 Å, C16′–H16A···O11′* 162.65°.

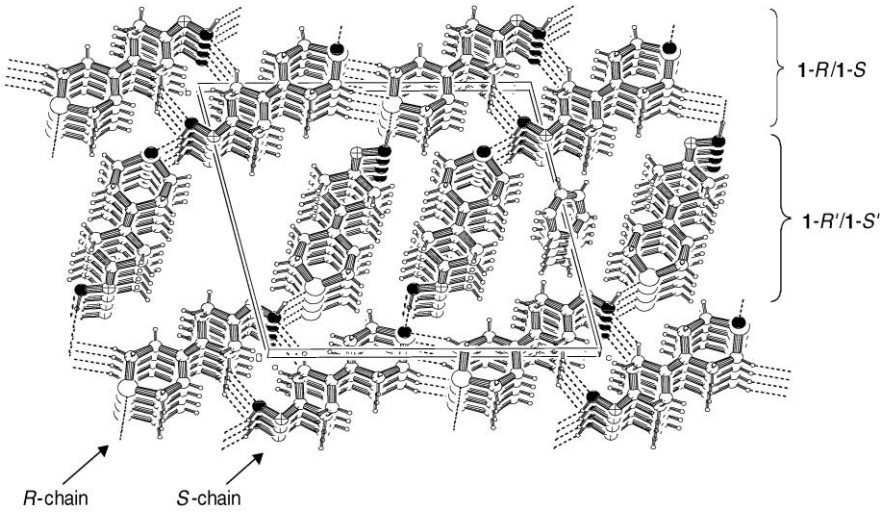

Fig. 6 Two-dimensional hydrogen bonding networks in **(1)$_4$·C$_6$H$_6$** stacked along the crystallographic direction [1 0 0]. The channels (area *ca.* 25 Å^2) contain C_6H_6 solvent molecules (for clarity the C_6H_6 molecules occupying the left hand channel of the unit cell have been omitted).

were further studied using thermal analysis [thermogravimetry [TGA(N_2)] and differential scanning calorimetry (DSC)] and solid-state IR and Raman spectroscopy. Compounds **1** and **(1)$_4$·C$_6$H$_6$** possess similar thermal properties, which differ markedly from those of **2–5**. Whereas **2–5** possess discrete melting points (DSC: **2**, 127 °C; **3**, 114 °C;[3c] **4**, 155 °C; **5**, 97 °C[8]) and evaporate at distinct temperatures [TGA(N_2): **2**, 150 °C; **3**, 125 °C;[3c] **4**, 150 °C; **5**, 160 °C], native **1** and **(1)$_4$·C$_6$H$_6$** have similar very high melting points [**1**, 199 °C; **(1)$_4$·C$_6$H$_6$**, 193 °C] and both decompose upon melting [onset of weight loss [TGA(N_2)]: **1**, 234 °C; **(1)$_4$·C$_6$H$_6$**, 200 °C]. This suggests that native, polycrystalline **1** and **(1)$_4$·C$_6$H$_6$** possess similar solid-state structures. Note that the TGA(N_2) curve of **(1)$_4$·C$_6$H$_6$** compared to that of **1** exhibits an extra (abrupt) weight loss of *ca.* 7% at 100 °C, which corresponds to an endothermic peak in the DSC curve (T_{onset} = 100.8 °C, ΔH = 43.1 kJ mol^{-1}). It is therefore attributed to the loss of C_6H_6 (C_6H_6: calc. 8%, found 7%) from **(1)$_4$·C$_6$H$_6$**.

For native **1** the occurrence and the nature of the intermolecular hydrogen bonding motifs in the solid-state were investigated in detail using IR and Raman spectroscopy (Table 1). As evidenced by the broad O–H stretching vibrations ($\nu_{O\text{–}H}$) and the absence of sharp vibrations characteristic for free O–H groups (*ca.* 3600 cm^{-1}) in the IR, the oxime units of native **1** participate in hydrogen bonding.[19] It is documented that mono-oximes **3** and **5** form centrosymmetric dimers (C_i-symmetry; intermolecular $R_2^2(6)$ oxime–oxime hydrogen bonding motifs), which possess characteristic IR and Raman vibrational signatures.[3] For example, the '*out-of-plane*' O–H···N vibration ($\gamma_{O\text{–}H}$) is diagnostic for the type of intermolecular oxime–oxime hydrogen bonding.[3] Whereas in IR $\gamma_{O\text{–}H}$ of trimeric aggregates is positioned at *ca.* 800 cm^{-1},[3] $\gamma_{O\text{–}H}$ of related dimeric aggregates is positioned at *ca.* 760 cm^{-1} (*cf.* **3** and **5**, Table 1). Furthermore, the '*in-plane*' O–H···N vibration ($\delta_{O\text{–}H}$) of these dimers, which is generally partially overlapped by CH_2 scissoring modes (1470–1430 cm^{-1}),[20] is found at lower wavenumbers in IR than in Raman ($\Delta\nu$, *ca.* 30 cm^{-1}).[21] This is a consequence of intermolecular coupling

§ $1-x, -y, 2-z$.
¶ $x, -1+y, z$.
* $2-x, -y, 1-z$.
†† $-1+x, y, 1+z$.

Table 1 Salient solid-state IR and Raman (between parentheses) data for $(\mathbf{1})_4\cdot\mathbf{C_6H_6}$, native, polycrystalline **1** and **2–5**.[19]

Vibration	$(\mathbf{1})_4\cdot\mathbf{C_6H_6}$/cm^{-1}	native **1**/cm^{-1}	**2**/cm^{-1}	**3**/cm^{-1}	**4**/cm^{-1}	**5**/cm^{-1}
ν_{O-H}	3550–3000 s	3500–3000 s	3350–3100 s	3500–3000 s	—	3500–3000 s
γ_{O-H}	770 w	760 w	756 w	760 w	—	763 w
$\nu_{C=N}$	1658[a] w	1657 w	1677 w	1675 w	—	1677 w
	(1658)[b] w	(1657)[b] w	(1668) w	(1669)[b] w	—	(1671) w
$\nu_{C=C}$	(1653)[b] s	(1649)[b] s	(1654) s	(1659)[b] s	(1655) s	—
$\nu_{S=O}$	1030 w	1032 w	—	—	1037 s	—
	1000 m	1007 s			1025 w	
	976 s	977 s			1012 s	
					1005 m	

[a] Band partially overlaps with very weak bands of C_6H_6 at 1618 and 1638 cm^{-1}. Pure C_6H_6: 1585 and 1606 cm^{-1}.[23] [b] In Raman the $\nu_{C=N}$ peaks appear as low intensity shoulders of the respective $\nu_{C=C}$ modes; the band maxima were determined *via* band-deconvolution.

of the two δ_{O-H} vibrations of the dimeric oxime hydrogen bonding $R_2^2(6)$ motif for which an '*in-phase*' and an '*out-of-phase*' mode is found. Since these motifs possess C_i-symmetry the former will be exclusively IR active and the latter exclusively Raman active (mutual exclusion principle).[22] Similar vibrational coupling accompanied by mutual exclusion in IR *vs.* Raman is also found for the $\nu_{C=N}$ stretch vibrations of **3** and **5** (Table 1).[23] Solid-state IR and Raman spectroscopy of **2** revealed that similar intermolecular dimeric oxime hydrogen bonding occurs as found for **3** and **5**.[3] In line with the intermolecular oxime–sulfoxide hydrogen bonding for $(\mathbf{1})_4\cdot\mathbf{C_6H_6}$ in the solid-state, the position of γ_{O-H} (770 cm^{-1}) differs from that of **2, 3** and **5**. Although at first sight in the case of native, polycrystalline **1**, the position of γ_{O-H} (760 cm^{-1}) suggests that intermolecular dimeric oxime hydrogen bonding occurs, the position of the $\nu_{C=N}$ peak (1657 cm^{-1}) shows that this hydrogen bonding motif cannot be present. For both $(\mathbf{1})_4\cdot\mathbf{C_6H_6}$ (1658 cm^{-1}) and native **1** $\nu_{C=N}$ (1657 cm^{-1}) is positioned at a significantly lower wavenumber ($\Delta\nu_{C=N}$ *ca.* 20 cm^{-1}) than that for **2**, **3** and **5** (Table 1). In fact, the $\nu_{C=N}$ vibrations of **1** and $(\mathbf{1})_4\cdot\mathbf{C_6H_6}$ are located at identical positions in IR and Raman. Intermolecular coupling of the $\nu_{C=N}$ vibration as a consequence of centrosymmetric, intermolecular dimeric oxime hydrogen bonding motifs is not observed. Therefore, the oxime moiety of native **1** has to participate in a different type of intermolecular hydrogen bonding in the solid-state, which resembles that found for $(\mathbf{1})_4\cdot\mathbf{C_6H_6}$. Further support is obtained from a comparison of the $\nu_{S=O}$ vibrations of native **1**, $(\mathbf{1})_4\cdot\mathbf{C_6H_6}$ and **4**. Although $\nu_{S=O}$ is strong in IR and shifts ($\Delta\nu_{S=O}$ 15–40 cm^{-1}) towards lower wavenumbers upon hydrogen bonding,[20] its assignment is generally hindered without the use of (selective) isotope labelling due to the complexity of $\nu_{S=O}$ absorption patterns (Table 1: **1**, 1032 − 1007 cm^{-1}; $(\mathbf{1})_4\cdot\mathbf{C_6H_6}$, 1030 − 976 cm^{-1}; **4**, 1037 − 1005 cm^{-1}).[24] Whereas in IR **4** possesses two strong absorption bands positioned above 1005 cm^{-1}, similar strong bands at *ca.* 1000 cm^{-1} are absent in the IR spectra of native **1** and $(\mathbf{1})_4\cdot\mathbf{C_6H_6}$. Temperature dependent IR spectroscopy revealed that during *in situ* heat treatment of $(\mathbf{1})_4\cdot\mathbf{C_6H_6}$ from 25 °C to 184 °C the hydrogen bond motifs remain intact, *i.e.* although all incorporated C_6H_6 is removed (*vide supra*), the characteristic vibrations assigned to the intermolecular oxime–sulfoxide hydrogen bonding motifs persist. Hence, we conclude that in the case of native **1** in the solid-state intermolecular oxime–sulfoxide hydrogen bonding occurs, which strongly resembles the hydrogen bonding motif found in the single crystal X-ray structure of $(\mathbf{1})_4\cdot\mathbf{C_6H_6}$.

Aggregation behaviour of 1–5 in solution

To gain insight in the aggregation behaviour of native **1** in solution, concentration-dependent IR measurements were performed for **1–3** and **5**. In $CDCl_3$[25] solution the IR spectra show that all compounds display the common aggregation behaviour, *i.e.* self-complementary intermolecular oxime–oxime hydrogen bonding.[26] Mixtures of free as well as aggregated molecules are observed. In line with expectation $\nu_{C=N}$ and ν_{O-H} of the hydrogen bonded species are positioned at higher and lower wavenumber, respectively (Table 2). Concomitant with increasing concentration the intensities of the peaks attributed to the aggregated species increase at the expense of those of the free molecules. Furthermore, the strong $\nu_{S=O}$ vibration of **1** is found at identical position as that of **4** (Table 2). Note that in CCl_4 solution $\nu_{S=O}$ of **4** is positioned at significantly higher wavenumbers than in $CDCl_3$ (Table 2). A similar shift to lower wavenumber in going from CCl_4 to $CDCl_3$ was found for $\nu_{S=O}$ of DMSO and tetrahydro-4*H*-thiopyran oxide ($\Delta\nu$ 15–40 cm^{-1}). This has been attributed to hydrogen bonding between the sulfoxide moiety (hydrogen bond acceptor) and $CDCl_3$ (hydrogen bond donor).[20,27] Thus in $CDCl_3$, the sulfoxides of **1** and **4** are hydrogen bonded to solvent molecules. As a consequence, **1** can only aggregate *via* its oxime groups.

To verify that different aggregation occurs if the sulfoxide groups cannot participate in hydrogen bonding with the solvent, a CCl_4 solution of mono-oxime **3** (0.1 M) containing both free and aggregated **3**, was titrated with DMSO.[25] With increasing amounts of DMSO, the intensity of ν_{O-H} of the free oximes (3604 cm^{-1}) decreases at the expense of that of ν_{O-H} of hydrogen bonded molecules (3265 cm^{-1}). Furthermore, the intensity of the $\nu_{C=N}$ peak of aggregated **3** (1669 cm^{-1}) decreases and is replaced by a new band positioned at lower wavenumber (1656 cm^{-1}), which is indicative for the occurrence of intermolecular oxime–sulfoxide hydrogen bonding (Fig. 7, spectra A to E). For comparison, the IR spectrum of a DMSO solution of **3** shows exclusively broad ν_{O-H} bands (hydrogen bonded O–H groups) and a $\nu_{C=N}$ peak positioned at 1654 cm^{-1}. Thus with

Table 2 Salient solution IR (solvent $CDCl_3$) data of **1–5**

Vibration		**1**/cm^{-1}	**2**/cm^{-1}	**3**/cm^{-1}	**4**/cm^{-1}	**5**/cm^{-1}
ν_{OH}	free	3589	3590	3590	—	3588
	aggregated	3500–3000	3500–3000	3500–3000	—	3500–3000
$\nu_{C=N}$	free	1658	1657	1657	—	1658
	aggregated	1668	1667	1666	—	1669
$\nu_{S=O}$	free	—	—	—	1058 CCl_4	—
	aggregated	1041/1015	—	—	1040 $CDCl_3$	—

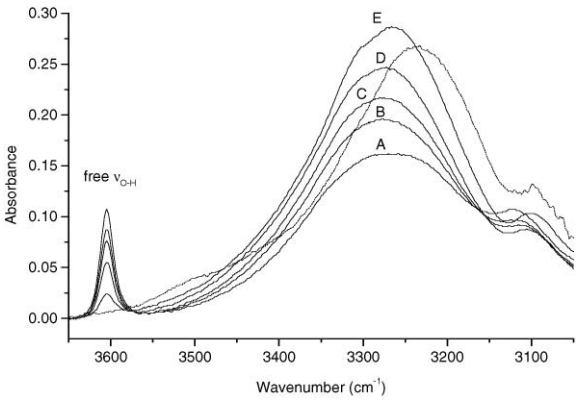

a

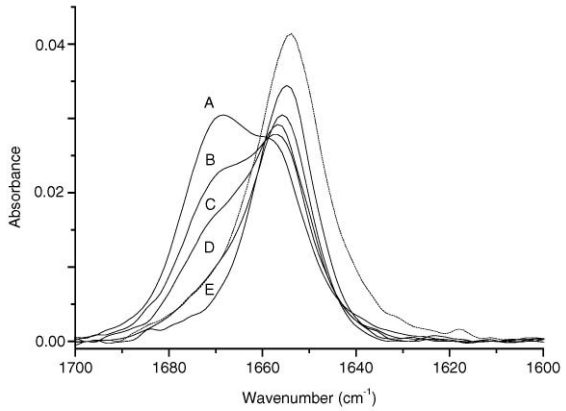

b

Fig. 7 Partial IR spectra of **3** showing the ν_{O-H} (a) and $\nu_{C=N}$ (b) regions (solvent CCl_4 0.1 M) after titration with DMSO (A, 0.00 M; B, 0.064 M; C, 0.130 M; D, 0.250 M; E, 0.50 M). The remaining dotted spectrum represents **3** in DMSO (0.1 M).

increasing amounts of DMSO, intermolecular oxime–sulfoxide hydrogen bonded aggregates replace the initial intermolecular oxime–oxime hydrogen bonded aggregates in solution. From spectrum C, where DMSO and **3** are present in a ratio 1 : 1, it is apparent that intermolecular oxime–sulfoxide hydrogen bonding is preferred. Note that in the case of intermolecular oxime–sulfoxide hydrogen bonding, the position of $\nu_{C=N}$ with respect to that in free oximes is nearly unaffected (*vide supra*). In contrast, $\nu_{C=N}$ experiences a significant shift towards higher wavenumber ($\Delta\nu_{C=N}$ *ca.* 14 cm^{-1}) upon intermolecular oxime–oxime hydrogen bonding.[28] Thus, while ν_{O-H} reflects the extent of hydrogen bonding taking place in solution, the position of the $\nu_{C=N}$ peak is diagnostic for whether the oxime group acts as a hydrogen bond donor or acceptor.

Conclusions

Racemic **1** (**1**-*R*/**1**-*S*) crystallizes as a co-crystal $\mathbf{(1)_4{\cdot}C_6H_6}$ ($P\bar{1}$ space group) from a saturated C_6H_6 solution. The unit cell contains two crystallographically independent enantiomer pairs **1**-*R*/**1**-*S* and **1**-*R*′/**1**-*S*′. In the solid-state **1** adopts a *syn*-conformation and form enantiomorphous, infinite non-covalent chains *via* '*head-to-tail*' intermolecular oxime–sulfoxide hydrogen bonding in the crystallographic direction [2 1 1]; each chain consists of either *R*- or the *S*-enantiomers in an alternating fashion, *viz.* **1**-*R* · · · **1**-*R*′ or **1**-*S* · · · **1**-*S*′. Hence, chiral molecular recognition occurs. The chains are interconnected *via* secondary weak C–H · · · O hydrogen bonding interactions between one of the crystallographically independent enantiomer pairs **1**-*R* and **1**-*S* *via* centrosymmetric C–H · · · sulfoxide $R_2^2(8)$ and C–H · · · oxime R_2^2 (12) motifs. As a consequence, a nearly planar two-dimensional network is formed. The layers are stacked in the crystallographic direction [1 0 0] giving channels (area: *ca.* 25 Å^2) in the same direction, which are occupied by C_6H_6 solvent molecules. The higher ring puckering disorder of the cyclohexyl-type rings of the crystallographic enantiomer pair **1**-*R*′/**1**-*S*′ and the C_6H_6 solvent molecules is accounted for by the absence of similar secondary interactions.

Based on a comparison of the IR and Raman data of native **1** and $\mathbf{(1)_4{\cdot}C_6H_6}$, it is concluded that also in the case of native **1** intermolecular oxime–sulfoxide hydrogen bonding occurs in the solid-state. In $CDCl_3$ **1** aggregates *via* its oxime groups due to preferred hydrogen bonding of its sulfoxide groups with the solvent. However, titration of mono-oxime **3** in CCl_4 with DMSO shows that intermolecular oxime–sulfoxide hydrogen bonding gradually replaces intermolecular oxime–oxime aggregation, *i.e.* intermolecular oxime–sulfoxide hydrogen bonding is preferred.

Experimental

General

NMR: Bruker AC 300 spectrometer (^{1}H, 300.13 MHz; ^{13}C, 75.44 Mhz) with $CDCl_3$ as solvent unless otherwise stated (internal standard: TMS). Solid-state FT-IR: Nicolet Magna-IR 860 spectrometer using KBr pellets (resolution: 1 cm^{-1}). Partly *O*-deuterated samples were prepared by dissolution of a small amount of material (*ca.* 25 mg) in CD_3OD (0.2 ml) followed by evaporation of the solvent *in vacuo*. Solid-state Raman spectra of neat materials: Perkin Elmer System 2000 FT-IR spectrometer equipped with a Raman accessory (resolution: 2 cm^{-1}). Solution FT-IR: Perkin Elmer System 2000 FT-IR spectrometer (resolution: 2 cm^{-1}). Samples were dissolved in $CDCl_3$ (Cambridge Isotope Laboratories, 99.8% D) and measured in liquid cells (path lengths 0.2 or 1 mm, NaCl windows). Samples were dried by overnight by storage in the presence of P_2O_5 in a vacuum desiccator. Powder wide-angle X-ray diffraction (WAXD): Delft Instruments Guinnier Johansson FR552 camera (room temperature, 1.5405 Å Cu–Kα radiation). Melting points: Mettler FP5/FP51 apparatus (uncorrected) or differential scanning calorimetry (DSC): Mettler DSC 12E (samples 1–3 mg in sealed Al pans, N_2 atmosphere, heating and cooling rate 5 °C min^{-1}). Thermogravimetric analyses (TGA): Perkin Elmer TGS-2 apparatus equipped with an AR-2 autobalance (N_2 atmosphere, temperature program: 20→850 °C heating rate 20 °C min^{-1}.). HPLC: Pharmacia Fine Chemicals Liquid Chromatography Controller LCC-500 equipped with two Pharmacia Fine Chemicals Liquid pumps P 3500, a Kratos Analytical Spectroflow 757 absorbance detector and a Diacel Chemical Industries Chiralcel OD column. (eluent: *n*-hexane–iso-propanol *v*/*v* 4 : 1), flow rate (1 ml min^{-1}.), UV detection (λ 218 nm). Elemental analyses: Dornis U. Kolbe, Microanalytisches Laboratorium, Mülheim a.d. Ruhr, Germany.

Syntheses

4-(Tetrahydro-4*H*-thiopyran-1-oxide-4-ylidene)cyclohexanone oxime (1). Prepared by stirring a mixture of **8** (216 mg, 1.02 mmol), $NH_2OH{\cdot}HCl$ (120 mg, 1.73 mmol), $NaHCO_3$ (110 mg, 1.31 mmol) and dry C_2H_5OH (4 ml) overnight at room temperature. Subsequently, the reaction mixture was diluted with water (7 ml) and extracted with $CHCl_3$ (3 × 10 ml). Crude **1** was obtained after drying (Na_2SO_4) of the combined $CHCl_3$ fractions and evaporation of the solvent *in vacuo*.

Recrystallization from $CHCl_3$–*n*-C_6H_{14} (*v*/*v* 1 : 1) afforded the pure product (172 mg, 0.76 mmol, 75%) as a white solid: mp 195 °C (dec.); ^{1}H NMR δ 2.36–2.60 (10H), 2.69–2.77 (2H), 2.86–2.93 (4H), 7.71 (1H) ppm; ^{13}C NMR δ 21.22, 21.31, 24.61, 25.59, 27.67, 30.13, 48.81, 49.06,126.65, 129.86, 160.06 ppm; FT-IR (KBr) ν_{max} 748, 923, 977, 1014, 1032, 1191, 1205, 1424, 1657, 2844, 2886, 2960, 3085, 3232 cm^{-1}; FT-Raman ν_{max} 631, 1008, 1031, 1225, 1312, 1409, 1436, 1650, 2890, 2917, 2967 cm^{-1}; anal. calc. for $C_{11}H_{17}NO_2S$: C, 58.12; H, 7.54; N, 6.16; O, 14.08; S, 14.10%, found: C, 57.96; H, 7.63; N, 6.07%.

4-(Tetrahydro-4*H*-thiopyran-4-ylidene)cyclohexanone oxime (2). Prepared according to the procedure described for **1**. Recrystallization of the crude material from $CHCl_3$–*n*-C_6H_{14} (*v*/*v* 1 : 1) gave pure **2** as a white solid (159 mg, 0.75 mmol, 83%): mp 127 °C; ^{1}H NMR δ 2.32–2.43 (6H), 2.53–2.67 (10H), 8.15 (1H) ppm; ^{13}C NMR δ 24.92, 25.49, 27.60, 30.36, 30.50, 30.63, 32.07, 32.13, 128.22, 129.76, 160.55 ppm; FT-IR ν_{max} 732, 760, 918, 963, 988, 1196, 1267, 1423, 1445, 1675, 2842, 2901, 2950, 2974, 3132, 3177, 3246 cm^{-1}; FT-Raman ν_{max} 660, 1021, 1217, 1307, 1426, 1456, 1510, 1654, 1668, 2893, 2953 cm^{-1}; anal. calc. for $C_{11}H_{17}NOS$: C, 62.52; H, 8.11; N, 6.63; O, 7.57; S, 15.17%, found: C, 62.50; H, 8.19; O, 7.32%.

4-Cyclohexylidene-tetrahydro-4*H*-thiopyran-1-oxide (4). Synthesized from 4-cyclohexylidene-tetrahydro-4*H*-thiopyran (**6**)[2] using the same procedure as used for **8**. The pure product was obtained after recrystallization from $CHCl_3$–*n*-C_6H_{14} (*v*/*v* 1 : 1) as a white crystalline solid (94 mg, 0.47 mmol, 81%): mp 155 °C; ^{1}H NMR δ 1.50–1.62 (6H), 2.20 (4H), 2.45–2.53 (2H), 2.72–2.93 (6H) ppm; ^{13}C NMR δ 21.38, 26.86, 28.46, 30.28, 49.70, 123.24, 134.44 ppm; FT-IR ν_{max} (KBr) 944, 1005, 1012, 1025, 1037, 1166, 1412, 1431, 1450, 2835, 2849, 2915, 2980 cm^{-1}; FT-Raman ν_{max} 623, 1219, 1322, 14.18, 14.39, 1655, 2925, 2986 cm^{-1}; anal. calc. for $C_{11}H_{16}OS$: C, 66.62; H, 9.15; O, 8.07; S, 16.16%, found: C, 66.49; H, 9.26; O, 7.93%.

1,1′-Bicyclohexylidene-4-one oxime (3)[3c,3d] and 4-cyclohexylcyclohexanone oxime (5)[8]. Prepared as described in detail elsewhere.

4-(Tetrahydro-4*H*-thiopyran-1-oxide-4-ylidene)cyclohexanone (8). Prepared by slow addition of a solution of 4-(tetrahydro-4*H*-thiopyran-4-ylidene)cyclohexanone[2] (**7**, 263 mg, 1.34 mmol) in CH_3OH (15 ml) to a solution of $NaIO_4$ (303 mg, 1.42 mmol) in water (9 ml)[7] at 0 °C. Subsequently, the resulting mixture was stirred for 3 h. at 0 °C and then warmed to room temperature. After addition of CH_3OH (9 ml) and stirring overnight, the reaction mixture was filtered and the residue washed with small amounts (10 ml) of CH_3OH and $CHCl_3$. The organic fractions were combined and after addition of water (25 ml) the product was extracted with $CHCl_3$ (3 × 25 ml). Drying (Na_2SO_4) of the combined organic layers and evaporation of the solvent *in vacuo* gave pure **8** (271 mg, 128 mmol, 96%) as a white solid: mp 182 °C; ^{1}H NMR δ 2.41–2.45 (4H), 2.53–2.68 (6H), 2.71–2.81 (2H), 2.90–2.97 (4H) ppm; ^{13}C NMR δ 21.16, 26.30, 39.92, 48.69, 127.60, 127.96, 211.40 ppm; FT-IR ν_{max} (KBr) 651, 765, 937, 987, 1013, 1035, 1198, 1244, 1274, 1297, 1352, 1419, 1445, 1472, 1700, 2842, 2887, 2959 cm^{-1}.

Single crystal X-ray determination of $(1)_4 \cdot C_6H_6$

Crystal data: formula, $2(C_{11}H_{17}NO_2S)\cdot\frac{1}{2}C_6H_6$; Triclinic P$\bar{1}$ No 2; *a*, 5.0885(3) Å; *b*, 15.5224(17) Å; *c*, 16.5379(16) Å; α, 102.839(8)°; β, 95.947(6)°; γ, 94.025(7); *V*, 1260.9(2) Å^3; *Z* = 2; Mw, 987.41; ρ_{calc} 1.3004(2) g cm^{-3}; X-ray data were collected for a colourless, cut-to-size plate (0.62 × 0.50 × 0.05 mm.) on an Enraf Nonius CAD4-T diffractometer (Rotating Anode; MoKα, λ = 0.71073 Å; $\theta_{max.}$ = 27.5°). A total of 7139 reflections were collected and averaged into a unique set of 5799 reflections [3386 with I > 2σ(I)]. Reflection profiles were relatively broad and structured, limiting the overall quality of the data set. The structure was solved by direct methods using SIR[29] and refined on F^2 by full matrix least squares using SHELXL97.[30] Hydrogen atoms were introduced at calculated positions and refined riding on the atoms to which they are attached. Convergence was reached at $R = 0.10$.‡‡

One of the cyclohexane rings (C1–C6, Fig. 4) showed some conformational/puckering disorder. No attempt was made to include this slight disorder effect in the refinement model. All geometrical calculations and the illustrations were done with PLATON.[31]

Semi-empirical PM3 calculations

Semi-empirical calculations were performed with MOPAC 7.0.[13] Geometry optimizations were done using the PM3 Hamiltonian; the Eigenvector following routine with initial Hessian calculation and increased convergence criteria (keywords: EF, HESS = 1, and PRECISE) were used; a GNORM < 0.03 was obtained. All minima were characterized by a Hessian calculation (keywords: FORCE and LARGE); no imaginary frequencies were found†.

Acknowledgements

Financial support in part (A. L. S.) by the Council for Chemical Sciences of the Netherlands Organization for Scientific Research (CW-NWO) is gratefully acknowledged.

References

1 (*a*) For general reviews: J.-M. Lehn, *Supramolecular Chemistry*, VCH, Weinheim, 1995; (*b*) G. R. Desiraju, *The Crystal as a Supramolecular Entity*, Wiley, New York, 1996; (*c*) E. Fan, C. Vicent, S. J. Geib and A. D. Hamilton, *Chem. Mater.*, 1994, **6**, 1113–1117; (*d*) D. Shekhar Reddy, Y. E. Ovchinnikkov, O. V. Shishkin, Y. T. Struchkov and G. R. Desiraju, *J. Am. Chem. Soc.*, 1996, **118**, 4085–4089 and references cited; (*e*) see the special issue on molecular networks in *New J. Chem.*, 1998, 87–210.

2 F. J. Hoogesteger, R. W. A. Havenith, J. W. Zwikker, L. W. Jenneskens, H. Kooijman, N. Veldman and A. L. Spek, *J. Org. Chem.*, 1995, **60**, 4375–4384.

3 (*a*) F. J. Hoogesteger, J. M. Kroon, L. W. Jenneskens, E. J. R. Sudhölter, T. J. M. de Bruin, J. W. Zwikker, E. ten Grotenhuis, C. H. M. Mareé, N. Veldman and A. L. Spek, *Langmuir*, 1996, **12**, 4760–4367; (*b*) E. ten Grotenhuis, A. W. Marsman, F. J. Hoogesteger, J. C. van Miltenburg, J. P. van der Eerden, L. W. Jenneskens, W. J. J. Smeets and A. L. Spek, *J. Cryst. Growth*, 1998, **191**, 834–845 and references cited; (*c*) F. J. Hoogesteger, L. W. Jenneskens, H. Kooijman, N. Veldman and A. L. Spek, *Tetrahedron*, 1996, **52**, 1773–1784; (*d*) A. W. Marsman, E. D. Leusink, J. W. Zwikker, L. W. Jenneskens, W. J. J. Smeets and A. L. Spek, *Chem. Mater.*, 1999, **11**, 1484–1491; (*e*) E. A. Bruton, L. Brammer, F. C. Pigge, C. B. Aakeröy and D. S. Leinen, *New. J. Chem.*, 2003, **7**, 1084–1094; (*f*) see also; M. Lutz, A. L. Spek, R. Dabirian, C. A. van Walree and L. W. Jenneskens, *Acta Cryst.*, 2004, **C60**, o127–o129.

4 A survey of single crystal X-ray structural data of 231 oxime derivatives in the Cambridge Crystallographic Database revealed that 54% gave this dimeric hydrogen bonding motif in the solid-state; V. Bertolasi, G. Gilli and A. C. Veronese, *Acta Cryst.*, 1982, **B38**, 502–511; L. Chertanova, C. Pascard and A. Sheremetev, *Acta Cryst.*, 1994, **B50**, 708–716.

5 M. C. Etter, *Acc. Chem. Res.*, 1990, **23**, 120–126; M. C. Etter, *J. Phys. Chem.*, 1991, **95**, 4601–4610.

6 M. Raban, D. Kost, W. B. Jennings and V. E. Wilson, in *Acyclic Organonitrogen Stereodynamics*, ed. J. B. Lambert and Y. Y. Takeuchi, VCH, Weinheim, 1991, pp. 57–88 and 177–193.

7 N. J. Leonard and C. R. Johnson, *J. Org. Chem.*, 1962, **27**, 282–284.

8 F. J. Hoogesteger, D. M. Grove, L. W. Jenneskens, T. J. M. de Bruin and B. A. J. Jansen, *J. Chem. Soc., Perkin Trans. 2*, 1996, 2327–2334.

9 N. S. Isaacs, *Physical Organic Chemistry*, Longman Group Limited, Essex, 1995, ch. 8, p. 351–368 and references cited.

‡‡ CCDC reference number 260603. See http://www.rsc.org/suppdata/ob/b5/b500527b/ for crystallographic data in CIF or other electronic format.

10 E. L. Eliel, S. H. Wilen and L. N. Mander, *Stereochemistry of Organic Compounds*, John Wiley and Sons, Inc., New York, 1994, ch. 14, p. 1119–1190.
11 The absolute configuration of an enantiomer of **1** (**1**-*R*/**1**-*S*) was determined by the relative orientation ofthe lone pairs and oxygen atoms of the nitrogen and sulfur atoms, respectively, from a Fisher projection along the chiral axis. For its configurational assignment see reference 4.
12 R. J. Abraham, L. Pollock and F. Sancassan, *J. Chem. Soc., Perkin Trans. 2*, 1994, 2329–2336 and references cited.
13 *MOPAC 7.0*, J. J. P. Stewart, 1993, PM3; J. J. P. Stewart, *J. Comp. Chem.*, 1989, **10**, 209–220.
14 R. W. A. Havenith, L. W. Jenneskens and J. H. van Lenthe, *Chem. Phys. Lett.*, 1998, **282**, 39–48.
15 A. Bondi, *J. Phys. Chem.*, 1964, **68**, 441–451.
16 For both contact distances: $d(D\cdots A) < R(D) + R(A) + 0.50$ Å, $d(\mathrm{H}\cdots A) < R(\mathrm{H}) + R(A) - 0.12$ Å and D–$\mathrm{H}\cdots A > 100.0°$, where R(x) are the van der Waals radii of the donor (D) and acceptor (A) atoms, respectively.
17 Weak C–H $\cdots$ O hydrogen bonds have been reported to be important and sometimes even dominant secondary interactions in, amongst others, molecular recognition processes, the determination of crystal packing and molecular conformations; T. Steiner, *Chem. Commun.*, 1997, 727–734 and references cited.
18 H. M. M. Shearer, *J. Chem. Soc.*, 1959, 1394–1397.
19 For the identification of the O–H group vibrations partially *O*-deuterated compounds were used (see Experimental).
20 For a general review: D. Lin-Vien, N. B. Colthup, W. G. Fateley and J. G. Grasselli, *The Handbook of Infrared and Raman Characteristic Frequencies of Organic Molecules*, Academic Press, San Diego, 1991.
21 In Raman the oxime $\delta_{\mathrm{O-H}}$ is the only active vibration of the O–H groups.
22 A similar coupling pattern in the IR is also observed for degenerate $\nu_{\mathrm{C=O}}$ vibrations of carboxylic acid dimers[20].
23 A comparison of the solid-state Raman spectra of native **1** and **(1)$_4$·C$_6$H$_6$** shows that the inclusion of C_6H_6 in the latter is supported by the presence of an additional strong (993 cm^{-1}) and weak (3062 cm^{-1}) absorption band, respectively. Their positions and intensity ratio are in agreement with those found for pure C_6H_6 (992 and 3062 cm^{-1}). *Cf.*, For a general review: F. R. Dolish, W. G. Fateley and F. F. Bentley, *Characteristic Raman Frequencies of Organic Compounds*, John Wiley and Sons, Inc., New York, 1974.
24 Generally, $\nu_{\mathrm{S=O}}$ of isolated free sulfoxide groups possess complex absorption patterns in the 1070–1037 cm^{-1} region.[20] See, for example, tetrahydro-4*H*-thiopyran oxide; T. Cairns, G. Eglinton and D. T. Gibson, *Spectrochim. Acta*, 1964, **20**, 159–167. An additional complicating factor is the overlap of the $\nu_{\mathrm{S=O}}$ and $\nu_{\mathrm{N-O}}$ (1000 − 900 cm^{-1}) absorption patterns.
25 Compound **1** is only sparingly soluble in CCl_4.
26 W. Luck, *Z. Elektrochem.*, 1961, **65**, 355–362.
27 M. Tamres and S. Searles, *J. Am. Chem. Soc.*, 1959, **81**, 2100–2104.
28 H. Saitô, K. Nukada and M. Ohno, *Tetrahedron Lett.*, 1964, **5**, 2124–2129, protonation of oximes preferably occurs at the nitrogen position.
29 A. Altomare, G. Cascarano, C. Giacovazzo and A. Guagliardi, *J. Appl. Cryst.*, 1993, **26**, 343–350.
30 G. M. Sheldrick, *SHELXL-97, Program for refinement of crystal structures*, University of Göttingen, Germany, 1997.
31 A. L. Spek, *J. Appl. Cryst.*, 2003, **36**, 7–13 and references cited.